Hindawi
Advances in Civil Engineering
Volume 2023, Article ID 3286769, 11 pages
https://doi.org/10.1155/2023/3286769

Research Article

Insights into Wall-Jet Scouring Characterization with the Kinect Device: Benefits and Limitations

Hadi Bali,[1] Seyed Hossein Mohajeri ,[2] and Amir Samadi[3]

[1]*Department of Civil and Water Engineering, Faculty of Science and Engineering, Azad University – Science and Research Branch, Tehran, Iran*
[2]*Department of Civil Engineering, Faculty of Engineering, Kharazmi University, No. 43, South Mofatteh Avenue, Tehran, Iran*
[3]*Department of Water Engineering, Faculty of Engineering and Technology, Imam Khomeini International University, Qazvin, Iran*

Correspondence should be addressed to Seyed Hossein Mohajeri; hossein.mohajeri@khu.ac.ir

Received 10 July 2022; Revised 21 June 2023; Accepted 27 June 2023; Published 14 July 2023

Academic Editor: Iacopo Carnacina

This study explores the use of the Kinect device for measuring Three-Dimensional (3D) Digital Elevation Models (DEMs) of wall-jet scour holes and its benefits and limitations. The Kinect device can accurately measure wall-jet scour holes in dry conditions with an accuracy of ±0.05 cm, but significant errors occur in the presence of water due to water surface refraction. A code based on Snell's law was developed to correct these errors, resulting in good agreement with point gauge measurements with an accuracy of ±0.12 cm. The method is not recommended for tail-water depth ratios smaller than three and densimetric Froude numbers larger than 7.75 due to water surface fluctuations. The findings have important implications for improving the efficiency and accuracy of scour hole measurements in hydraulic engineering, particularly for submerged wall-jet scouring, and the developed code can also be applied to other optical measurement devices.

1. Introduction

Accurately measuring bed elevations is crucial for monitoring natural or artificial conditions in erodible boundaries and for accurately simulating the flow field around movable beds. In ocean engineering, local scour holes are a significant problem and a common cause of structure failure [1, 2]. Therefore, it is essential for designers to have a comprehensive understanding of scour hole dimensions before constructing prototypes. Physical modeling and simulation of the scour process in a laboratory setting are commonly used to predict consequences and design hydraulic structures [3, 4]. To achieve accurate monitoring of scour at high spatial and temporal resolutions, various techniques have been developed and implemented, as described in studies by Tafarojnoruz et al. [4], Ballio and Radice [5], and Porter et al. [6].

In laboratory studies, accurate measurement of the bed topography of a scour hole caused by a 3D wall jet is essential for understanding the scour process and designing hydraulic structures. Previous research has identified four major methods for monitoring scour in laboratory settings: the point gauge, laser scanner, different photogrammetric methods, and echo-sounder [1, 7–9]. The point gauge, being the simplest method, has been commonly used in laboratory studies for many years. However, this method has several limitations, including its inability to measure the entire scour hole instantly, its time-consuming process, and its unsuitability for use in dynamic conditions (when the jet is on). With advances in technology, researchers are now using laser scanners to measure scour hole profiles, which offer highly accurate measurements [10–12]. However, the high cost of the device and the need for a precise traversing system are the main concerns associated with this method.

In recent years, computer science advancements have led to the development of innovative methods of creating 3D models of surfaces, such as image processing. Traditional photogrammetric methods require high costs and several ground control points, but new improvements have led to novel photogrammetric techniques, including PROSCAN (Profile Scanning) and Structure From Motion (SFM) [13–15]. PROSCAN can detect the scour profile and water surface, but it can only produce a two-dimensional scour

hole. SFM, on the other hand, works by employing the depth information generated by comparing the visual fields of two overlapping images. As the camera moves, objects around it move different amounts depending on their distance from the camera. SFM uses this depth information to generate a three-dimensional topography of objects [15]. Although SFM is an efficient method for generating Digital Elevation Models (DEMs), it faces challenges in the presence of a water surface.

The Kinect device, originally developed as a video game console by Microsoft in 2010, has recently emerged as a promising low-cost, high-resolution, short-range 3D/4D camera imaging system for measuring complex surface morphology. The Kinect device is a low-cost, high-resolution, short-range 3D/4D camera imaging system that has become popular in various disciplines due to its unique characteristics [16]. The device is supported by red, green, and blue (RGB) and infrared (IR) wavelength cameras, along with an IR emitter, which makes it efficient in dark environments compared to other imaging techniques. The portability and light weight of the Kinect device make it user-friendly and a practical option for acquiring bathymetry data, especially in coastal zones [17, 18]. Although some similar devices have been developed with similar characteristics, Microsoft is the first and only manufacturer of the Kinect device. The potential of the Kinect device for measuring natural water has been demonstrated by Klopfer et al. [19], who showed its applicability in investigating the statistical properties of surface waves [20].

The potential of the Kinect device for measuring complex surface morphology has been demonstrated by Bento et al. [21], who used it to measure the scour hole around an oblong bridge pier. The authors reported reliable and accurate estimates of scour hole topographic measurements using the Kinect device, but note that its applicability in the presence of water level is a significant limitation in their estimation. Chourasiya et al. [22] also employed the Kinect device to characterize irregular bed DEMs in the presence of a water surface and investigated the effects of different parameters, such as water turbidity, object color, and flow depth, on the constructed DEM using the Kinect device. They used Snell's law for refraction correction of underwater measurements and showed that the Kinect device is suitable for measurement in the presence of a water surface. However, all of their experiments were limited to uniform flow conditions.

The main objective of this study is to investigate the applicability of the Kinect device for measuring scour hole characteristics in nonuniform flow conditions caused by 3D wall jets. Unlike uniform flows, nonuniform flow conditions, such as wall jets, can cause significant water surface fluctuations that can affect the accuracy of the Kinect device measurements and require careful consideration. In tradition, scour hole characteristics are measured by draining the flume and using a point gauge, which may not provide an accurate representation of the actual scour hole shape and size [23]. In this study, the Kinect device will be used to measure scour hole characteristics in the presence of water before draining the flume, providing a more accurate representation of the scour hole under nonuniform flow conditions. The study will examine the effects of different parameters, such as tail-water depth ratio and densimetric Froude number, on the accuracy of the Kinect measurements. By analyzing the data collected from the experiments, this study aims to provide insights into the applicability of the Kinect device for measuring scour hole characteristics in nonuniform flow conditions caused by 3D wall jets. The results of this study have the potential to provide a new, more accurate method for measuring scour hole characteristics in nonuniform flow conditions, which can be useful for various engineering and scientific applications. Overall, this study represents a crucial step toward improving our understanding of scour hole characteristics and developing more efficient and accurate techniques for their measurement.

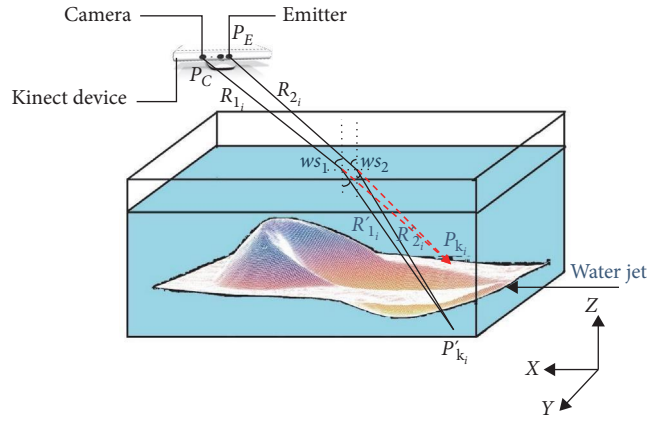

FIGURE 1: Schematic view of 3D Snell's law application for scour hole refraction correction.

2. The Snell's Law Application

The presence of water surface above the scour hole can produce significant errors due to light refraction, which should be corrected based on Snell's law [24]. To correct the obtained DEM of the Kinect device, the locations of the Kinect's emitter and camera and the water surface must be clear. Let P_E and P_C be the locations of the Kinect's emitter and camera, respectively, and let P_{K_i} be a desirable bed point measured by the Kinect device. Figure 1 shows these parameters, along with other variables and parameters that will be used in deriving the equations.

For each point (P_{K_i}), the Kinect device send a ray toward the bed from the emitter to an object (R_{1_i}) and receive a ray from object to the camera (R_{2_i}). The vectors of R_{1_i} and R_{2_i} can simply derived based on the P_{K_i},P_E, and P_C using (Equations 1 and 2):

$$R_{1_i} = P_E - P_{K_i}, \tag{1}$$

$$R_{2_i} = P_C - P_{K_i}. \tag{2}$$

To find the corrected location of the bed point P'_{K_i}, both of the rays needs refraction correction. The corrected rays are shown by R'_{1_i} and R'_{2_i}. The corrected rays can be obtained using the vector of the Snell's law in 3D space which can be represented as

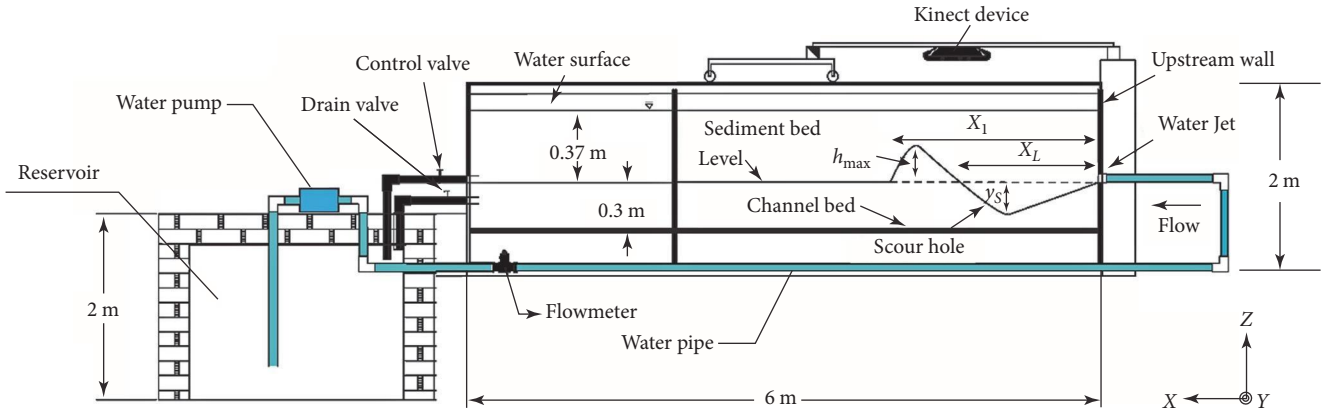

FIGURE 2: Schematic view of the experimental set-up together with scour hole parameters.

$$R'_{1_i} = \frac{n_a}{n_w}\left[\widehat{N}_{ws_1} \times \left(-\widehat{N}_{ws_1} \times R_{1_i}\right)\right] - \widehat{N}_{ws_1}\sqrt{1 - \left(\frac{n_a}{n_w}\right)^2 . \left(\widehat{N}_{ws_1} \times R_{1_i}\right) . \left(\widehat{N}_{ws_1} \times R_{1_i}\right)}, \tag{3}$$

$$R'_{2_i} = \frac{n_a}{n_w}\left[\widehat{N}_{ws_2} \times \left(-\widehat{N}_{ws_2} \times R_{2_i}\right)\right] - \widehat{N}_{ws_2}\sqrt{1 - \left(\frac{n_a}{n_w}\right)^2 . \left(\widehat{N}_{ws_2} \times R_{2_i}\right) . \left(\widehat{N}_{ws_2} \times R_{2_i}\right)}, \tag{4}$$

where n_a and n_w are the refractive indices of air and water and $\widehat{N}_{ws_1}$ and $\widehat{N}_{ws_2}$ are the normal vector of the water surface for rays R_{1_i} and R_{2_i}, respectively. In this study, the experiments were conducted in asymptotic condition in which the water turbidity is almost negligible. Therefore, the refractive index of pure water ($n_w = 1.33$) has applied. To determine P'_{K_i}, one should determine the coordinates of the points of both ray's intersection to the water surface by WS_1 and WS_2 in Figure 1. Using the water surface elevation, Z_{ws} and R'_{1_i},R'_{2i} vectors, the lateral and streamwise coordinates of WS_1 and WS_2 can be determined. Finally, it is clear that P'_{K_i} is the location where the vectors of R'_{1_i},R'_{2i} intersect. Based on this fact and the coordinates of the WS_1 and WS_2 is the coordinate of P'_{K_i} can be simply determined. To correct the bed based on this algorithm a simple code has been written in MATLAB. The results obtained using this code will be shown in the Results section.

3. Laboratory Apparatus

The experiments were conducted in a recirculating open-channel flume that was 6 m long, 0.9 m wide, and 0.8 m deep at the Hydraulic Laboratory of Kharazmi University which can be seen in Figure 2. A sluice gate at the end of the open channel and a control valve were used to regulate the tail-water depth. Flow discharge was measured using a calibrated electromagnetic flowmeter (MagAb 3000). The tail-water depth and the bottom of the channel bed elevations were measured using a digital point gauge with a resolution of 0.01 mm. A carriage was used to transport the digital point gauge and Kinect device in the streamwise and spanwise directions. To estimate the uncertainty of the measurements using the point gauge, error analysis was employed, applying the central limit theorem and a significance level of 95%, which showed that the point gauge measurement uncertainty was ±0.2 mm. The streamwise and spanwise measurements were conducted using two rulers with a resolution of 1 mm, as shown in Figure 2. In this study, a right-handed coordinate system was used. The x-coordinate was oriented along the main flow, positive downstream, and parallel to the channel bed. The z-coordinate referred to the vertical direction, pointing upward from the initial position of the channel bed, and the spanwise y-axis was directed to the left wall from the wall-jet position. Thus, the origin of the coordinate system was located at the position of the wall jet (see Figure 2).

Before performing the experiment, the sands (sediments) were poured into the flume uniformly and up to a certain level (30 cm in this study). Additional attention considered to ensure that the sediments cover all areas of the flume and are uniformly distributed. The sediments were compacted slightly with a light weight and their surface were smoothed with a trowel. To create a wall-jet flow, water was pumped from a downstream tank into a 2 m long steel square pipe. The inner dimension of the pipe (D) was 2.5 cm and installed at the bottom of the channel to produce a submerged wall jet. A plate was used to protect the sediment bed level during regulating the tail-water depth and flow discharge. The plate removed slowly to let the scour process. Bed was covered using the sediment with $d_{50} = 2.15$ mm and $\sigma_g = \sqrt{d_{84}/d_{16}} = 1.18$ where d_i, is the bed material diameter, i % of which is finer by the weight and σ_g is the geometric standard deviation. To

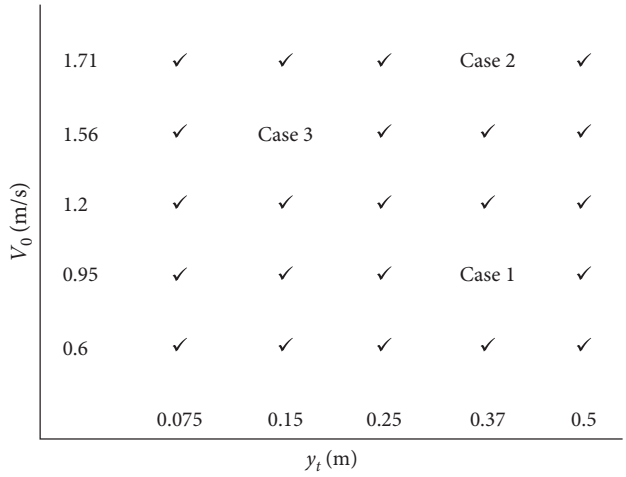

FIGURE 3: Hydraulics characteristics of measurements scenarios.

acquire sediment transport equilibrium condition, the wall jet has been flowed to the channel for 24 hr. After 24 hr from the scour process initiation, the scour hole reaches to the asymptotic state. In the asymptotic state, the scour hole dimensions did not change significantly with time [23]. Hence, the variation of the scour hole dimensions was negligible during the measurements in the wet conditions.

In this study, an Xbox 360 Kinect sensor with an RGB camera resolution of 1280×1024 pixels was used to produce the scour hole DEM. The Kinect also has a depth camera resolution of 640×480 pixels. The field of view (FOV), which is the open observable area for the Kinect device, was 57° horizontally and 43° vertically. This device can capture depth and color images simultaneously at a frame rate of up to 30 fps [25]. The Kinect device was fixed on a movable cart in a way such that the cameras and emitter were situated perpendicularly to the flume bed (see Figure 2). The device was located at coordinates of (35, 0, 107 cm). The device location was selected to ensure that the entire scour hole and ridge could be seen on the selected boundaries of the Skanect software. The boundaries were determined by a cubic with a 110 cm side in Skanect settings while the DEMs were created. During the measurement, it was observed that the Kinect device showed a complete black zone when the distance between the device and the bed was lower than ~70 cm. It is recommended that in each scour problem, researchers change the distance between the Kinect device and the bed to avoid the black zone.

To explore the accuracy of the results of the Kinect, 25 hydraulic scenarios were covered. Hydraulic characteristics of the experiments are reported in Figure 3. Five different tail-water depths (y_t) are selected to examine the importance of this parameter on the observed results. It is also highlighted that as the wall jet in this study is submerged, the water depth at the channel entrance is similar to tail-water depth. In addition, five wall-jet velocity (V_0) are covered during the experiment.

The measurements were conducted under two different conditions: the wet condition and the dry condition. In the wet condition, the jet was on, and the scour hole was observed in the presence of the water surface level. As point gauge measurements can disturb the natural conditions of the sediment bed and scour hole, measurements were only conducted using the Kinect device in the wet condition. The Kinect device was able to measure the scour hole in the wet condition as the scour holes had reached an asymptotic state. In contrast, measurements in the dry condition were conducted using both the point gauge and the Kinect device. During the measurement in the dry condition with the point gauge, the elevations of the sediment bed were recorded at a minimum interval of 1 cm in the streamwise and spanwise directions. The total time required to record the scour hole in the wet condition was 12 min. In contrast, the required time to measure the scour hole topography using the point gauge was over 7 hr. Therefore, point gauge measurements for each scour hole took about 42 times longer than the Kinect device measurements. In addition, the obtained mesh using the point gauge was too coarse in comparison to the Kinect device.

4. Results and Discussion

In Figure 4, the DEM models of scour hole for Case 1 in the wet condition, before and after refraction correction are shown. The effects of the presence of the water surface are clear in Figure 4(a). More precisely, a concave curve is detected beyond the perimeter of the scour hole where, in the real case condition, $z = 0$ cm. The refraction correction (Figure 4(b)) improves the measurements of the DEM. CV is used as a parameter to find the effect of the refraction correction on the main scour hole parameters quantitatively and defined as Equation (5).

$$CV_{\varphi} = 100|(\varphi_{\mathrm{BRC}} - \varphi_{\mathrm{ARC}})/\varphi_{\mathrm{ARC}}|, \tag{5}$$

where φ_{BRC} and φ_{ARC} are the target parameter such as scour hole characteristics (y_s, $h_{\max}$, X_L, W, and X_t) or sediment bed level (zl) before and after refraction correction, respectively. Table 1 shows the CV_{φ} for different parameters of the main scour hole characteristics in Case 1.

It is clear that the refraction affects all scour hole characteristics. This is more obvious on the vertical characteristics of the scour hole such as y_s and $h_{\max}$.

The author's observations before applying refraction correction show that generally the DEM model level was higher near the channel sidewall. Near the channel sidewall, in some points CV_{zl} reached 2,200 as zl values were very small after refraction correction. Generally, CV_{zl} increases as one goes from the centerline of the scour hole to the perimeter of the scour hole. The trend is due to two reasons. 1. Smaller values of the zl for the points that is far from the thalweg of the scour hole and 2. the location of the Kinect device during the measurements and the angle of the points respect to the device is also affects CV_{zl} values.

Figure 5 shows the DEM model for Case 1 using point gauge (Figure 5(a)), Kinect device in dry condition (Figure 5(b)) and Kinect device in wet condition (Figure 5(c)). The comparison of Figure 5(a) with Figures 5(b) and 5(c) clearly shows that the DEM mesh of the point gauge is too coarse in comparison to Kinect measurement. In addition, the point gauge

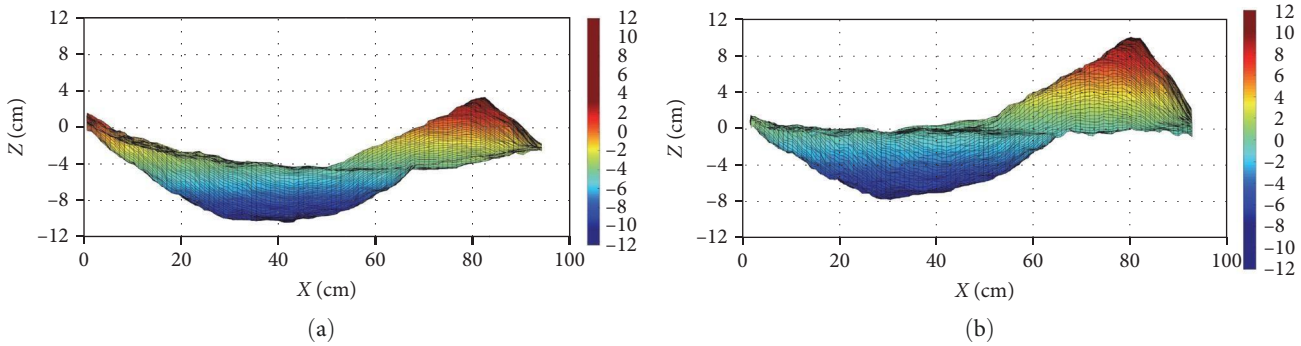

Figure 4: A sample 3D view of Digital Elevation Models (DEMs) of scour hole for Case 1 with water level presence (a) before refraction correction and (b) after refraction correction.

Table 1: CV_{φ} for different scour hole characteristics in Case 1.

φ	y_s	$h_{\max}$	X_L	W	X_t
CV	25	60	25	35	7

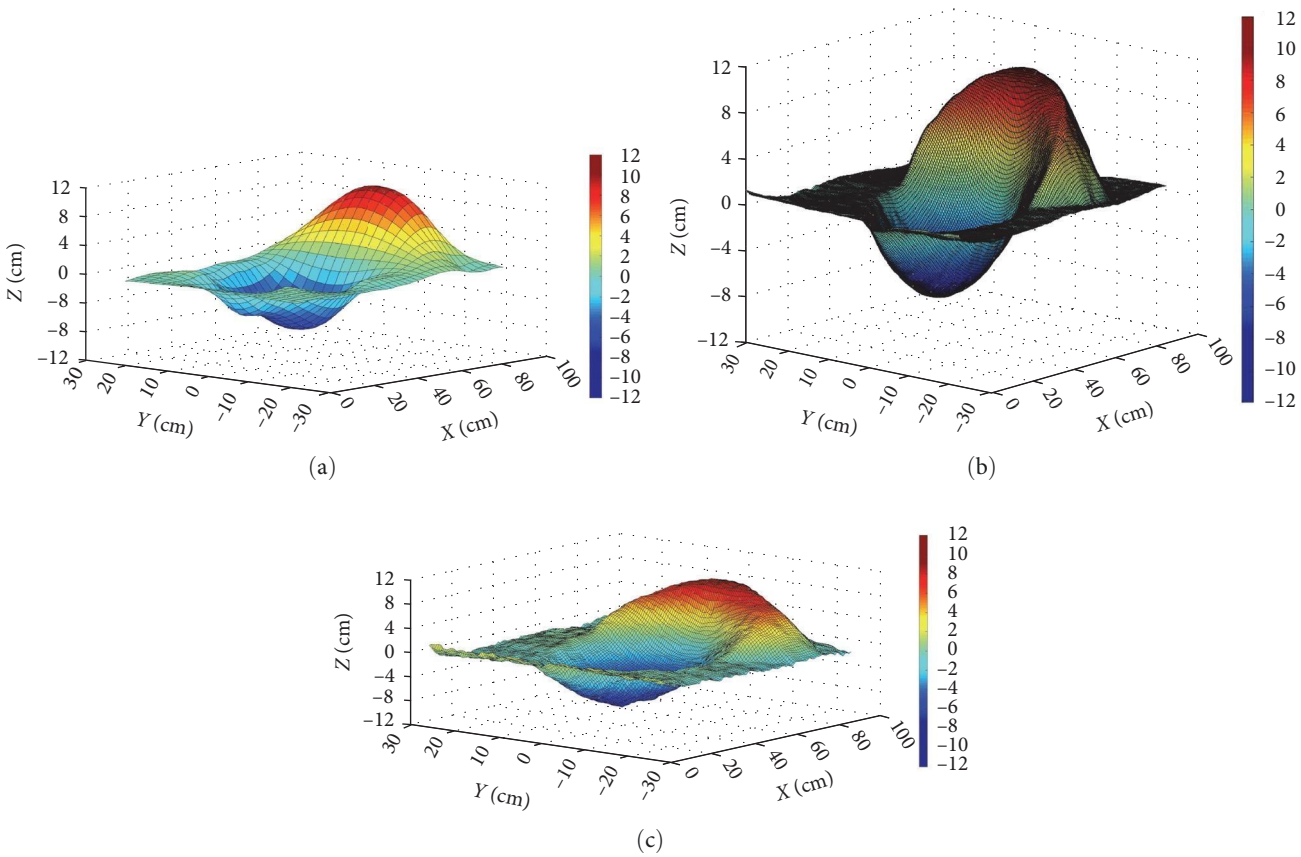

Figure 5: A DEM models of scouring hole for Case 1 using (a) point-gauge, (b) Kinect device for dry condition, and (c) Kinect device for wet condition after refraction correction.

measurements are a much more time-consuming process (7 hr) with such a coarse mesh. Comparison of the Kinect in wet and dry conditions expresses that generally, the quality of the obtained mesh in dry conditions is higher than the wet condition. After refraction corrections, the shape of the scour hole using Kinect device measurements in wet condition coincides well with the DEM models in Figures 5(a) and 5(b). The noises occurred due to the fixed position of the Kinect device in wet condition measurements and water surface fluctuation. However, the moving Kinect during the measurement in dry condition improves the quality of the measurements. The movement of Kinect device in wet condition was not possible as for

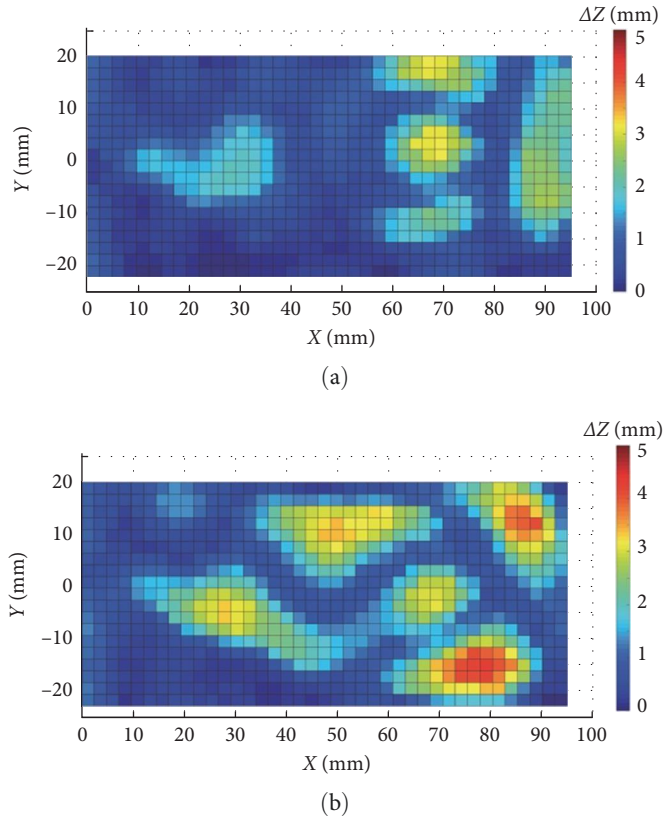

Figure 6: The absolute difference of point gauge measurement and Kinect measurements (a) dry condition and (b) wet conditions.

the correction using Equations (3) and (4) and the availability of the exact position of Kinect device is necessary. The total time duration in Kinect device measurements and analyzing the data for dry and wet conditions were 12 and 20 min, respectively.

To evaluate the performance of the Kinect device in estimating bed topography, the absolute difference between the Kinect device measurements and the point gauge measurements (Δz) in the wet and dry conditions were calculated and shown in Figure 6. The figure demonstrates a fair agreement between the Kinect measurements and point gauge measurements. Specifically, the mean absolute difference in bed topography between the Kinect measurements and point gauge measurements in the dry condition was 2% of the maximum sediment bed elevations, whereas in the wet condition, it was 8% of the maximum sediment bed elevations. The higher local noise present in the wet condition, as shown in Figure 5(c), resulted in a higher percentage of difference in the wet condition compared to the dry condition.

In the study of the scour hole, some geometrical characteristics of the scour hole and ridge are essential, including the maximum ridge height, longitudinal and transversal profiles of the scour hole, and maximum scour hole height. Figure 7 presents the maximum scour depth profile (Figure 7(a)) and the maximum ridge height profile (Figure 7(b)) along with the longitudinal scour hole in the centerline of the scour hole (Figure 7(c)) in both wet condition (black line) and dry condition (black dashed line) for Case 1. The results of some point gauge measurements are also shown by solid dashed line dots in Figure 7 for comparison. It is evident that the profiles match well with the point gauge data. Moreover, there is a good agreement between the Kinect device data in the dry condition and wet condition after refraction correction. Similar to Figure 5, Figure 7 shows some noise in the scour hole profiles for the wet condition, which is negligible in the dry condition.

To quantitatively compare the results of wet and dry conditions, in Table 2, the values of the most important geometrical characteristics of the scour hole composed of scour hole volume (V), maximum scour hole depth (y_s), width of scour hole (W), and length of scour hole (X_L) are reported and compared with the point gauge data measurement. These parameters are also shown in Figure 2. In Table 2, the error means the relative error which has been obtained using Kinect measurements as observed value and point gauge measurement as correct value. The reported errors of all scour hole characteristics in Case 1 are in the range of 0.6%–7%. The maximum error is for the scour hole length and scour hole width. This is may be due to the uncertainty of the measurements in longitudinal and transvers directions in addition to error in vertical direction. More precisely, there are two main sources of error in defining the scour hole length and width: 1. The small accuracy of the measurement device (which is in the case of the present study a meter with 1 mm resolution) in longitudinal and transverse directions and 2. the small slope of the downstream face of the scour hole and side wall of the scour hole. The latter makes some difficulties in determining the exact location of the $z = 0$ in transverse and longitudinal directions. In addition, a small difference between the Kinect device measurements and point gauge measurements in

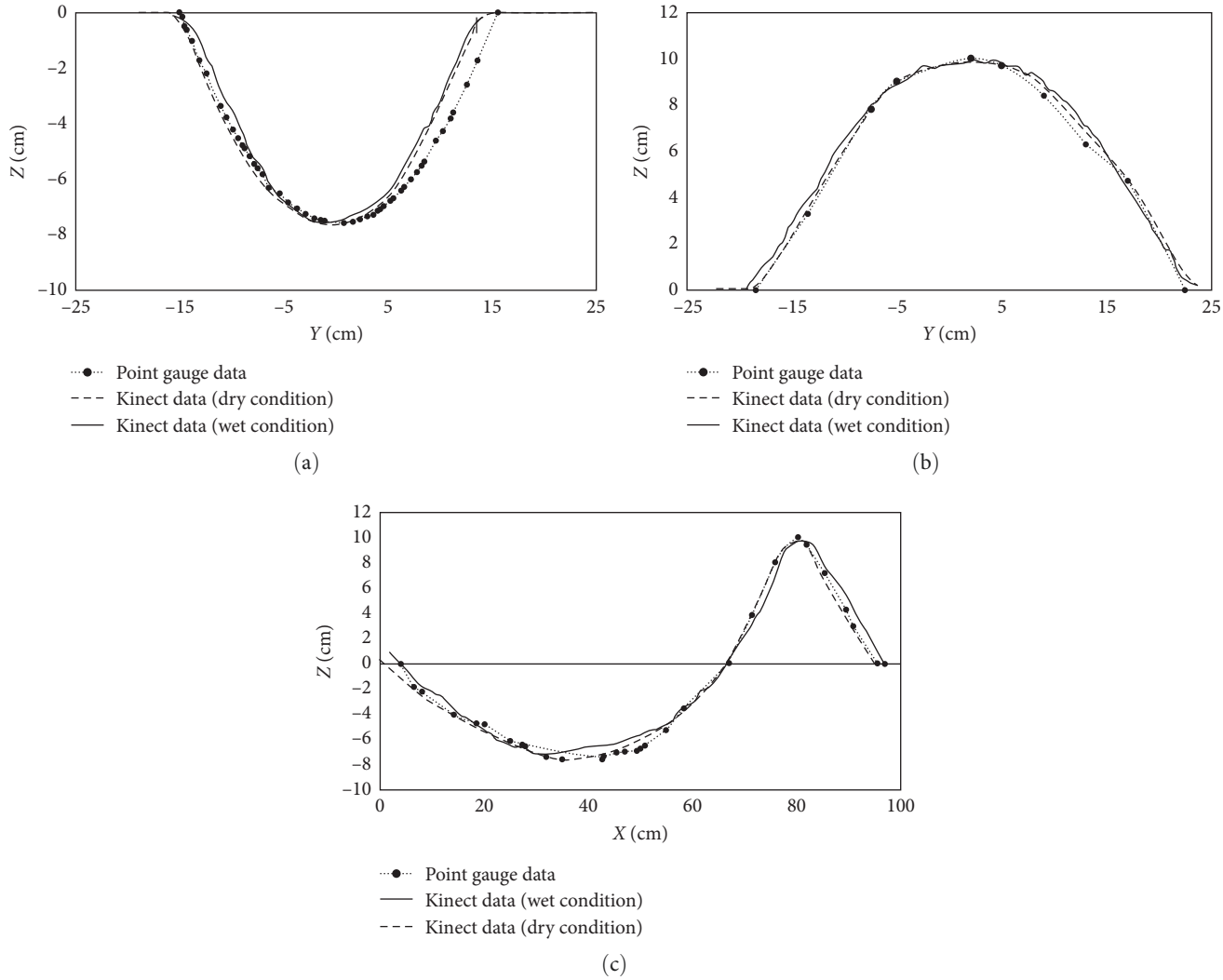

Figure 7: Comparison of results of Case 1 for (a) transversal profiles in maximum scour hole depth, (b) transversal profiles in ridge crest, and (c) longitudinal profiles in centerline of the scour hole.

Table 2: Scour-hole characteristics comparison through Kinect device for different hydraulic scenarios.

Name	Condition		V (cm^3)	h_{max} (cm)	y_S (cm)	W (cm)	X_L (cm)
Case 1	Wet conditions	Value	5350	9.94	−7.55	26.73	62.53
		Error (%)	3.2	0.6	0.66	7	3.88
	Dry conditions	Value	5230	9.84	−7.6	29.5	64.42
		Error (%)	1.1	1.62	1.32	3.4	6.7
Case 2	Wet condition	Value	2200	7.8	−5.8	20.5	51.91
		Error (%)	6.7	1.26	1.75	11.22	5.41
Case 3	Wet condition	Value	2870	6.7	−4.9	20.6	52.8
		Error (%)	9.1	4.28	2	6.8	7

maximum scour hole depth and the maximum ridge height can be observed. The maximum error of the scour hole characteristics reaches 11% and 9% in Case 2 and Case 3, respectively, which is slightly more than the error in Case 1.

To give some idea about the accuracy of the Kinect in other hydraulic conditions, Figures 8(a) and 8(b) show the DEM models for Case 2 and Case 3. Comparisons between the results of Case 1 (Figure 5(c)) with Case 2 (Figure 8(a)) clarifies the effects of the tail-water depth on scour hole measurements using Kinect device in the wet condition. In addition, a comparison between Case 1 (Figure 5(c)) and Case 3 (Figure 8(b)) improves our knowledge about the effects of the jet velocity on scour hole measurements using Kinect device in the wet condition. Similarly, in Case 1 (Figure 5(c)) some

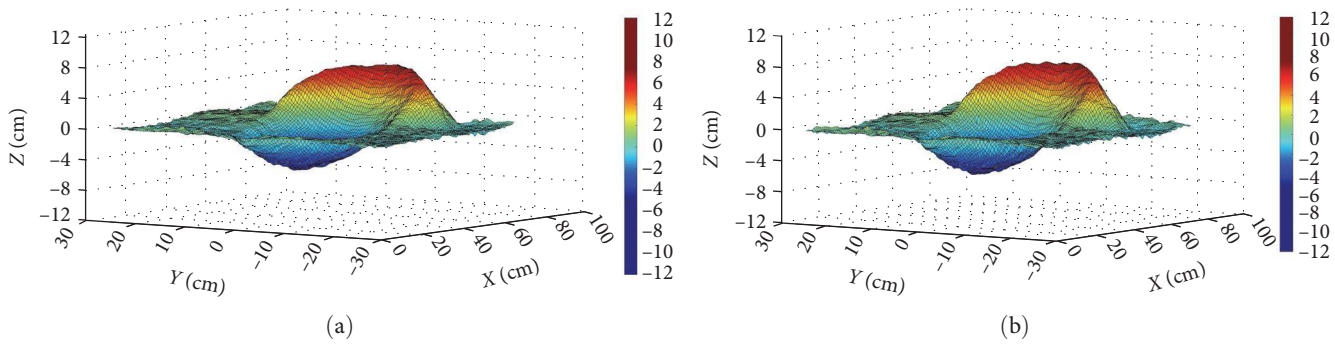

Figure 8: Contour maps of obtained DEM models of scour hole for other hydraulic conditions (a) Case 2 and (b) Case 3.

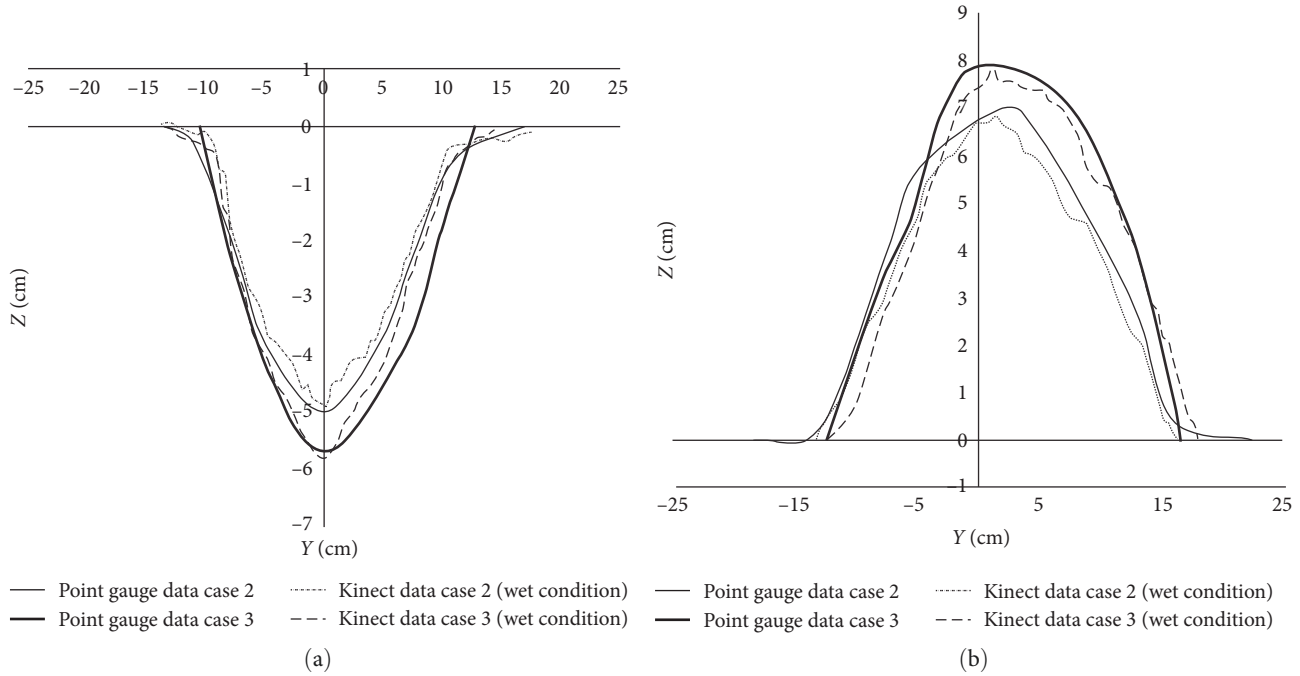

Figure 9: Transversal profiles using Kinect device in presence of water level for Case 2 and Case 3: (a) scour hole and (b) scour ridge.

noises can be observed in acquired DEM models. The noises are more pronounced in Case 2 and Case 3 compared to Case 1. Smaller tail-water depth and larger jet velocity in Case 2 and Case 3 compared to Case1 make larger water surface fluctuations that makes stronger noises in Case 2 and Case 3.

Figure 9 shows the transverse profiles of the scour hole in the maximum scour depth location (Figure 9(a)) and maximum ridge height locations (Figure 9(b)) for Case 2 and Case 3. It is obvious that the Kinect measurement error of the profiles increased as compared to Case 1. The noises are more obvious in Case 2 and Case 3. The main reason for such a difference can be associated with the smaller water depth in Case 3 in comparison to Case 1. In addition, in both Case 2 and Case 3 the wall-jet velocity is higher than that in Case 1. This observation expresses that any increase in wall-jet velocity and any decrease in the depth of tail-water can increase the error of the estimated geometrical characteristics obtained by the Kinect device.

To describe the overall quality of collected data, the accuracy of the system for the hydraulic conditions of measurements has been estimated. The absolute error, for all the points that point gauge data are available, are calculated. The results show that for Case 1, Case 2, and Case 3 in wet condition, the absolute error in estimation of bed topography is respectively ± 0.3, ± 0.6, and ± 0.5 cm. In addition, for the dry condition, the absolute error is ± 0.1 cm which is lower than the obtained values for the wet conditions. It is also important that the spatial resolution of the measured topography using Kinect device in horizontal plane (i.e., in x- and y- directions) is almost 1 mm.

Previous studies regarding wall jet show that tail-water depth ratio (y_t/D) and densimetric Froude number, ($Fr_d = V_o/\sqrt{1.65(gd_{50})}$, where g is the acceleration of gravity), are the main parameters in wall-jet scour hole modeling [1]. To explore these parameter impacts on y_s, h_m, W, and X_T, point gauge and Kinect measurements for 25 experiments

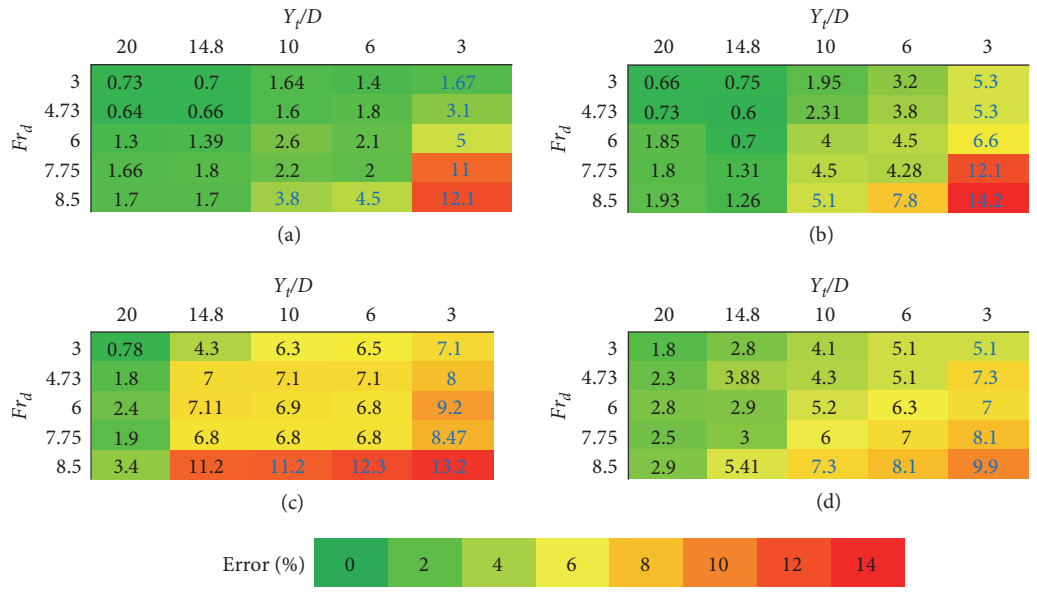

FIGURE 10: Error matrices for different parameters of (a) y_s, (b) h_m, (c) W, and (d) X_L.

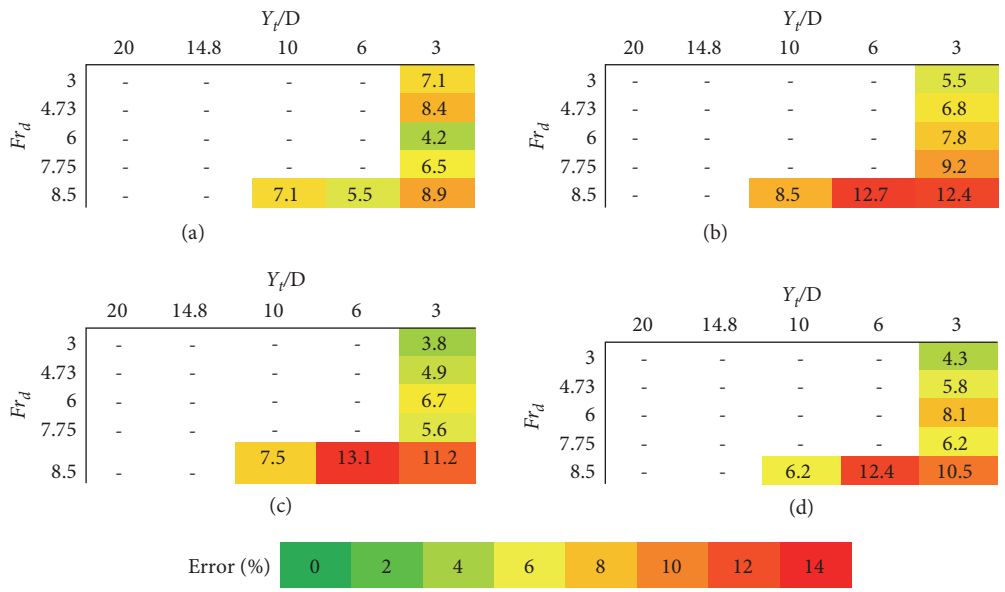

FIGURE 11: Error matrices for different parameters, (a) y_s, (b) h_m, (c) W, and (d) X_L, using box to eliminate the wavy water surface.

(Figure 4) are compared and reported in Figure 10. For all scour hole dimensions, the maximum error occurs at the lowest tail-water depth and maximum densimetric Froude number (i.e., e_{55} where e_{ij} is the entry of the i^{th} row and j^{th} column of the matrix). The average error of all experiments for y_s, h_m, w_s, and X_L are 2.7%, 3.9%, 6.8%, and 5%, respectively. The lowest error in scour hole dimensions' measurement is detected in y_s and the error of Kinect device in h_m measurement is slightly larger than y_s. This is attributed to the wavy water surface which affects the results of the ridge height measurement using Kinect device. The flow deviation toward the water surface after flow collision to the downstream face of the scour hole makes strong waves on the water surface. The wave on the water surface amplified in low tail-water depth ratio and high-densimetric Froude number and as a result the maximum error occurred for $y_t/D = 3$ and $Fr_d = 8.5$.

To produce DEM using the Kinect, it is also possible to put the device in a water proof box and locate the box and Kinect below the water surface. Using this approach on Kinect measurement, the effects of the wavy water surface was eliminated on scour measurement. This approach has been satisfactorily employed by Klopfer et al. [19] to mitigate the DEM production error. In this study, the performance of this approach on wall-jet scour hole characterization is checked. The results of the differences of the scour hole dimensions with and without the box presence are presented in (Figure 11). It should be noted that these experiments are

conducted only for those experiments in Figure 10 with blue color font. It is clear that the presence of the box increases the maximum scour hole dimension.

This is due to the deviation of the flow toward the bottom of the scour hole after jet collision to the bottom of the box which was reported as digging phase by Bey et al. [1]. The ridge height h_m also increases due to the increases of the sediment removing from the scour hole. The maximum difference between the two conditions (using box on the water surface and without using box on the water surface) reaches to 8.9%, 12.7%, 13.1%, and 12.4% for y_s, h_m, W, and X_L, respectively. As a general trend, the difference of scour hole dimension with and without box increases in higher Fr_d.

5. Conclusions

The traditional method of measuring scour hole characteristics using a point gauge is time-consuming and does not allow for the study of temporal variations caused by wall jets in wet conditions. The Kinect device was explored as an alternative method for determining the bed elevations of scour holes due to wall jets in laboratory experiments conducted in both dry and wet conditions. Although the Kinect device was found to provide accurate results in dry conditions, water refraction effects caused significant errors in wet conditions. A code was developed to correct these errors in 3D, improving the accuracy of the bed elevation measurements. However, the obtained DEM for the wet condition measurements showed noises primarily due to water surface fluctuations. Increasing the densimetric Froude number and decreasing the tail-water depth ratio increased the effects of noises on the measurement of scour hole dimensions using the Kinect device. Therefore, the method is not recommended for tail-water depth ratios smaller than 3 and densimetric Froude numbers larger than 7.75, due to the significant water surface fluctuations during the measurements.

This study has several limitations that should be taken into consideration when interpreting the results. First, the experiments were conducted in a laboratory flume under controlled water flow and bed conditions. As a result, the applicability of the Kinect device in field conditions and different flow and bed conditions remains to be investigated. In addition, the code developed to correct the water refraction effects in the Kinect measurements was based on certain assumptions about the water surface and the properties of the Kinect device. It is possible that these assumptions may not be valid under different conditions. Therefore, further research is needed to validate the accuracy of the correction method under a wider range of flow and bed conditions.

Despite these limitations, the Kinect device has significant advantages over traditional methods for measuring scour hole characteristics, such as low cost sensors, the ability to provide high-quality 3D models with low errors, and the ability to develop rapid real-time 3D models. The results of this study can contribute to the development of improved and more efficient techniques for measuring scour hole characteristics in laboratory conditions, which can have significant implications for hydraulic engineering and related scientific applications.

Data Availability

The data that support the findings of this study are available from the corresponding author upon reasonable request.

Conflicts of Interest

The authors declare that they have no conflicts of interest.

References

[1] A. Bey, M. A. A. Faruque, and R. Balachandar, "Effects of varying submergence and channel width on local scour by plane turbulent wall jets," *Journal of Hydraulic Research*, vol. 46, no. 6, pp. 764–776, 2008.

[2] R. Gaudio, A. Tafarojnoruz, and F. Calomino, "Combined flow-altering countermeasures against bridge pier scour," *Journal of Hydraulic Research*, vol. 50, no. 1, pp. 35–43, 2012.

[3] A. Tafarojnoruz, R. Gaudio, and F. Calomino, "Bridge pier scour mitigation under steady and unsteady flow conditions," *Acta Geophysica*, vol. 60, pp. 1076–1097, 2012.

[4] A. Tafarojnoruz, R. Gaudio, and F. Calomino, "Evaluation of flow-altering countermeasures against bridge pier scour," *Journal of Hydraulic Engineering*, vol. 138, no. 3, pp. 297–305, 2012.

[5] F. Ballio and A. Radice, "A non-touch sensor for local scour measurements," *Journal of Hydraulic Research*, vol. 41, no. 1, pp. 105–108, 2003.

[6] K. E. Porter, R. R. Simons, and J. M. Harris, "Laboratory investigation of scour development through a spring-neaptidal cycle," in *7th International Conference on Scour and Erosion*, CRC Press, Perth, Western Australia, 2014.

[7] M. Fazli, M. Ghodsian, and S. A. A. S. Neyshabouri, "Scour and flow field around a spur dike in a 90° bend," *International Journal of Sediment Research*, vol. 23, no. 1, pp. 56–68, 2008.

[8] M. Ghodsian, M. Mehraein, and H. R. Ranjbar, "Local scour due to free fall jets in non-uniform sediment," *Scientia Iranica*, vol. 19, no. 6, pp. 1437–1444, 2012.

[9] M. Ebrahimi, P. Kripakaran, D. M. Prodanović et al., "Experimental study on scour at a sharp-nose bridge pier with debris blockage," *Journal of Hydraulic Engineering*, vol. 144, no. 12, Article ID 04018071, 2018.

[10] Z. Zhang, "Microsoft Kinect sensor and its effect," *IEEE MultiMedia*, vol. 19, no. 2, pp. 4–10, 2012.

[11] S. Akib, A. Jahangirzadeh, and H. Basser, "Local scour around complex pier groups and combined piles at semi-integral bridge," *Journal of Hydrology and Hydromechanics*, vol. 62, no. 2, pp. 108–116, 2014.

[12] G. Dodaro, A. Tafarojnoruz, G. Sciortino, C. Adduce, F. Calomino, and R. Gaudio, "Modified einstein sediment transport method to simulate the local scour evolution downstream of a rigid bed," *Journal of Hydraulic Engineering*, vol. 142, no. 11, Article ID 04016041, 2016.

[13] R. Balachandar and J. A. Kells, "Instantaneous water surface and bed scour profiles using video image analysis," *Canadian Journal of Civil Engineering*, vol. 25, no. 4, pp. 662–667, 1998.

[14] M. J. Westoby, J. Brasington, N. F. Glasser, M. J. Hambrey, and J. M. Reynolds, "'Structure-from-Motion' photogrammetry: a low-cost, effective tool for geoscience applications," *Geomorphology*, vol. 179, pp. 300–314, 2012.

[15] S. Ullman, "The interpretation of structure from motion," *Proceeding of the Royal Society B*, vol. 203, no. 1153, pp. 405–426, 1979.

[16] K. D. Mankoff and T. A. Russo, "The Kinect: a low-cost, high-resolution, short-range 3D camera," *Earth Surface Processes and Landforms*, vol. 38, no. 9, pp. 926–936, 2013.
[17] T. Butkiewicz, *Low-Cost Coastal Mapping using Kinect V2 Time-of-Flight Cameras*, Oceans - St. John's, NL, Canada, 2014.
[18] L. I. Nicholson, M. Pętlicki, B. Partan, and S. MacDonell, "3-D surface properties of glacier penitentes over an ablation season, measured using a Microsoft Xbox Kinect," *The Cryosphere*, vol. 10, no. 5, pp. 1897–1913, 2016.
[19] F. Klopfer, M. Hämmerle, and B. Höfle, "Assessing the potential of a low-cost 3-D sensor in shallow-water bathymetry," *IEEE Geoscience and Remote Sensing Letters*, vol. 14, no. 8, pp. 1388–1392, 2017.
[20] F. Toselli, F. De Lillo, M. Onorato, and G. Boffetta, "Measuring surface gravity waves using a Kinect sensor," *European Journal of Mechanics - B/Fluids*, vol. 74, pp. 260–264, 2019.
[21] A. M. Bento, L. Couto, J. P. Pêgo, and T. Viseu, "Advanced characterization techniques of the scour hole around a bridge pier model," *E3S Web of Conferences*, vol. 40, Article ID 05066, 2018.
[22] S. Chourasiya, P. K. Mohapatra, and S. Tripathi, "Non-intrusive underwater measurement of mobile bottom surface," *Advances in Water Resources*, vol. 104, pp. 76–88, 2017.
[23] M. Mehraein, M. Ghodsian, and S. A. A. Salehi Neyshaboury, "Local scour due to an upwards inclined circular wall jet," *Proceedings of the Institution of Civil Engineers - Water Management*, vol. 164, no. 3, pp. 111–122, 2011.
[24] Y. A. Garbovskiy and A. V. Glushchenko, *A Practical Guide to Experimental Geometrical Optics*, Cambridge University Press, 2017.
[25] K. Khoshelham and S. O. Elberink, "Accuracy and resolution of Kinect depth data for indoor mapping applications," *Sensors*, vol. 12, no. 2, pp. 1437–1454, 2012.